Smith, T.M., Saylor, J.E., Lapen, T.J., Leary, R.J., and Sundell, K.E., 2022, Large detrital zircon data set investigation and provenance mapping: Local versus regional and continental sediment sources before, during, and after Ancestral Rocky Mountain deformation: GSA Bulletin, https://doi.org/10.1130/B36285.1.

Supplemental Material

Supplemental Material 1. Alternate source map, outliers, sample descriptions, and appendices references.

Supplemental Material 2. New and previously published detrital zircon metadata table.

Supplemental Material 3. New detrital zircon U-Pb reduction data.

Supplemental Material 4. Detrital zircon *DZnmf* run table.

Supplemental Material 5. *DZnmf* 30 source runs export for samples and sample groups (i.e., N=191 results).

Supplemental Material 6. *DZmix* and *DZnmf* results summary for 11 sources used in paper, and 11 sources plus 1.085 Ga source sample (12 sources).

Supplemental Material 7. Paleocurrent metadata table.

Supplemental Material 8. *DZnmf* 30 source runs export for individual samples (i.e., N=329 results)

Supplemental Material 9. *DZmix* Matlab code that allows for multiple samples to be loaded at one time and run. This uses the same algorithm as *DZmix* (Sundell and Saylor, 2017). See test run file for format of input. Make sure to put sample data first, then sink data. Number of sources, bandwidth, iterations, etc.

SUPPLEMENTAL MATERIAL 1:

Supplemental Materials Table of Contents:

Alternate source map version

11 source set plus 1085 Ma source *DZmix* results

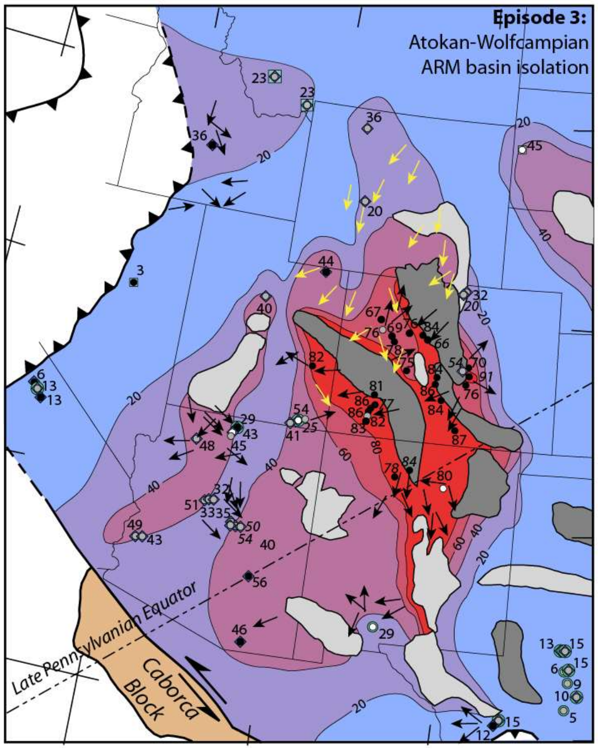

Episode 3 provenance map similar to Fig.8C, but *DZmix* data points were modeled with the 11-source set plus a 1.085 Ga unimodal source to represent detritus shed from the Pike's Peak Batholith. This granitoid exhibits a unique age for intraplate intrusive rocks in central Colorado (Fig. 7) because it is commonly associated with a series of 1.3-0.95 Ga intrusive complexes that were primarily emplaced along the eastern and southern margin of Laurentia during the Grenville Orogeny (Whitmeyer and Karlstrom, 2007). Note the increase of local sediment in the central proximal Denver Basin., but also an increase in in samples on the Wyoming, Montana, and Arizona shelves (See Fig. 8 for legend)

Figure data references

Figure 8

A) Episode 1: Paleogeography from Gehrels et al. (2011). Stratal thickness and zero Mississippian thickness line (white with tick marks) are from Carlson (1999).

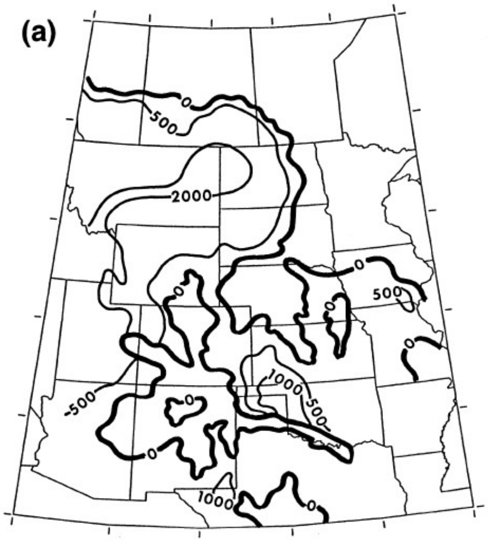

Carlson (1999), figure 3A.

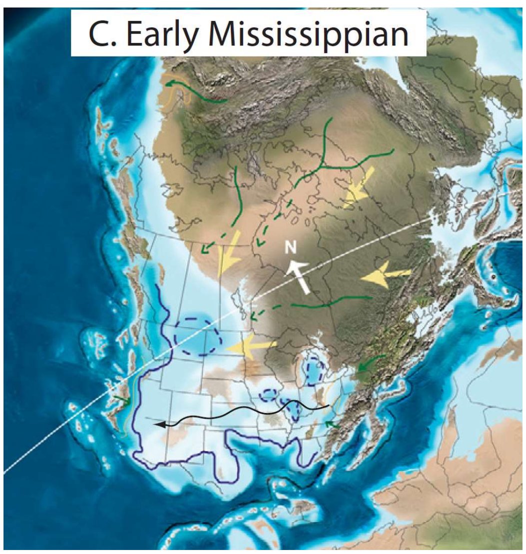

Gehrels et al. (2011) figure 10C.

B) Episode 2: Paleogeography (Ye et al., 1996; Gehrels et al., 2011), and paleocurrent data (Billingsley and Beus, 1999; Bowen and Weimer, 2003; Gleason et al., 2007; Wang and Bidgoli, 2019)

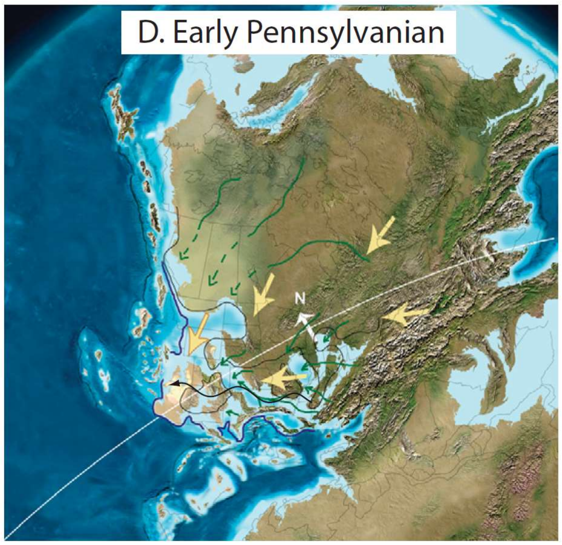

Gehrels et al. (2011) figure 10D.

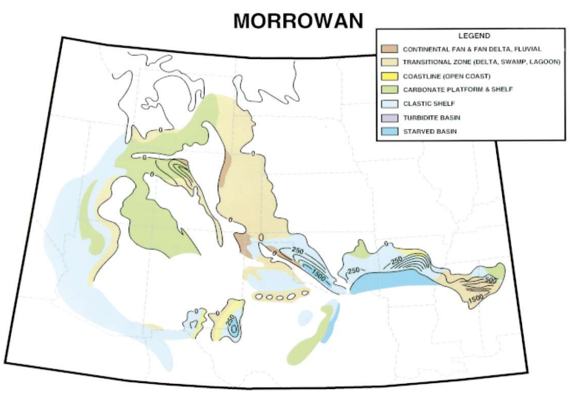

Ye et al. (1996) figure 2B.

C) Episode 3: Paleogeography (Ye et al., 1996; Blakey, 2009; Gehrels et al., 2011; Lawton et al., 2017), stratal thickness maps (Ye et al., 1996; Blakey, 2009), and paleocurrent data (Opdyke and Runcorn, 1960; Johnson, 1987; Geslin, 1998; Soegaard and Caldwell, 1990; Eberth and Miall, 1991; Gleason et al., 2007; Sweet and Soreghan, 2010; Lawton et al., 2015; this study) were used in map construction.

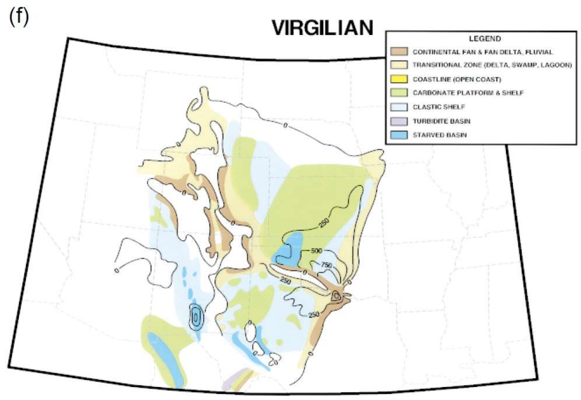

Ye et al. (1996) figure 2F.

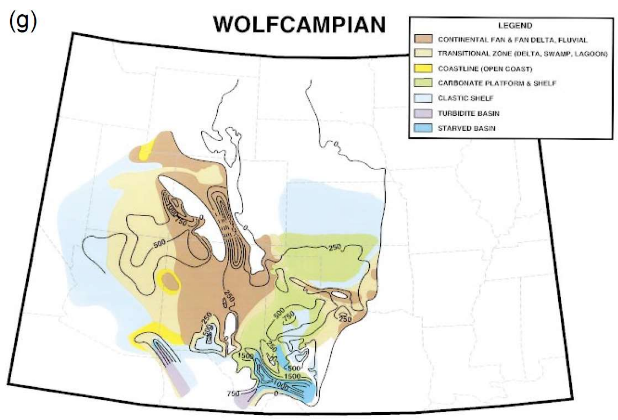

Ye et al. (1996) figure 2G.

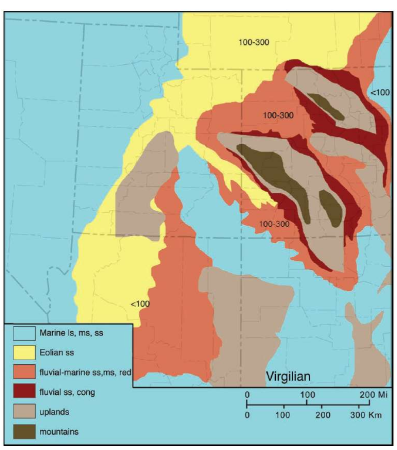

Blakey (2009) figure 14A.

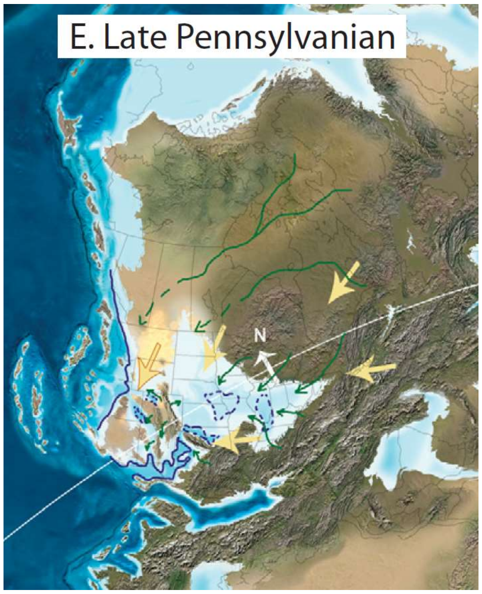

Gehrels et al. (2011) figure 10E.

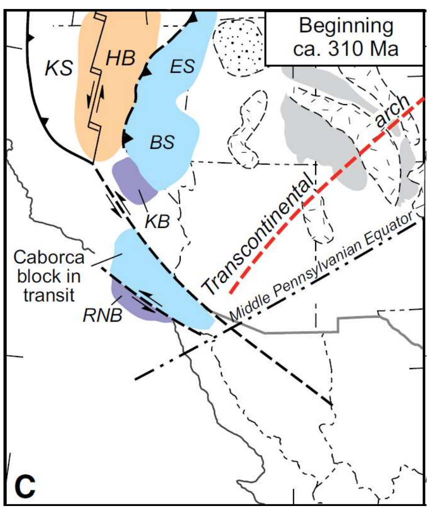

Lawton et al. (2017) figure 1C.

D) Episode 4: Paleogeography (Loope et al., 2004; Leary et al., 2017), stratal thickness maps (Ewing, 1993; Ye et al., 1996), and paleocurrent data (McKee, 1940; Rea, 1967; Conyers, 1975; Adams, 1980; Loope et al., 2004; Lawton et al., 2015; Brand et al., 2015; Dickinson, 2018) were used in map construction.

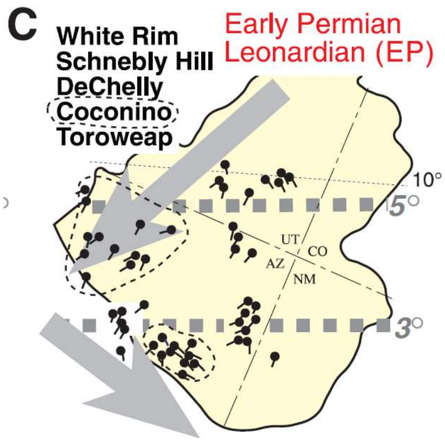

Loope et al., 2004

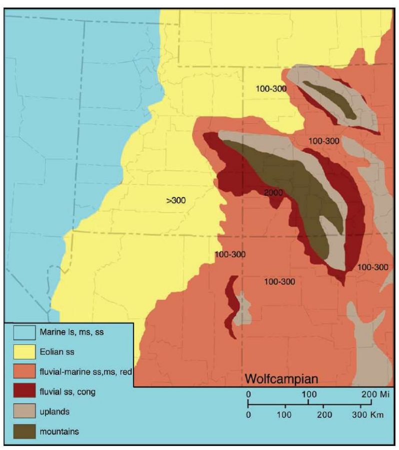

Blakey (2009) figure 15A.

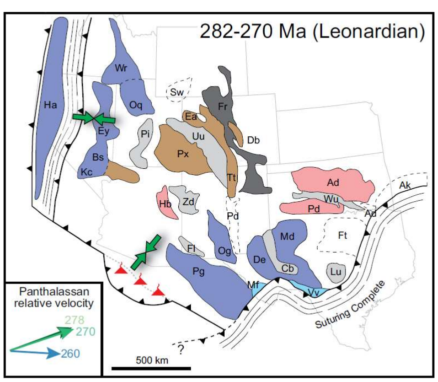

Leary et al. (2017) figure 2.

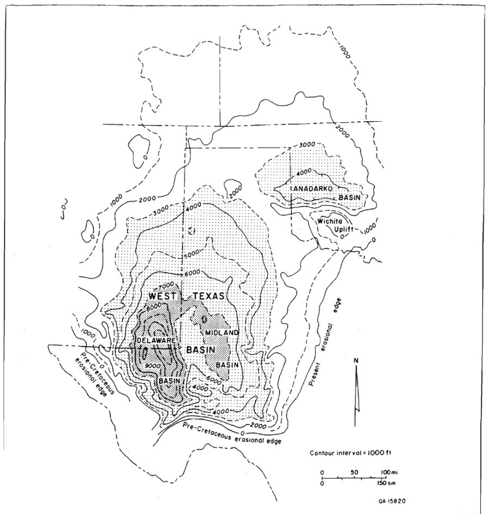

Ewing (1993) figure 2.

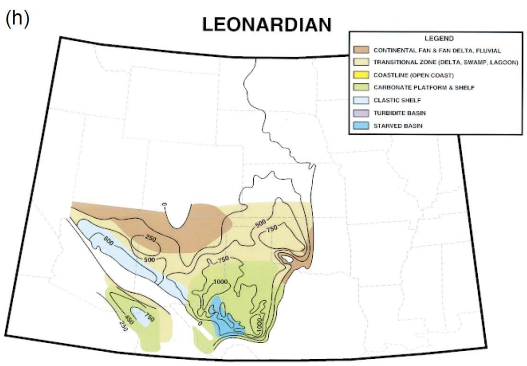

Ye et al. (1996) figure 2H.

E) Episode 5: Paleogeography (Dickinson and Gehrels, 2008; Lawton et al., 2018), stratal thickness maps (Dickinson and Gehrels, 2008; Kent and Irving, 2010), and paleocurrent data (Willis, 1967; Harms and Williams, 1988; Dickinson and Gehrels, 2008; Brand et al., 2015; Riggs et al., 2016; this study) were used in map construction.

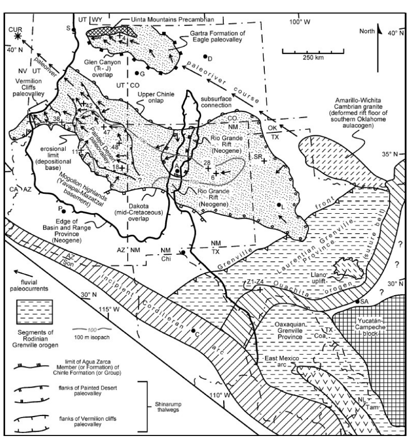

Dickinson and Gehrels (2008) figure 4.

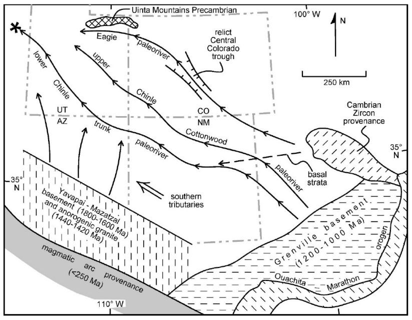

Dickinson and Gehrels (2008) figure 15.

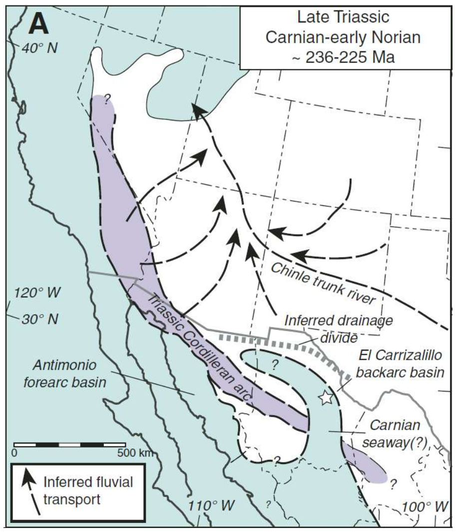

Lawton et al. (2018) figure 13A

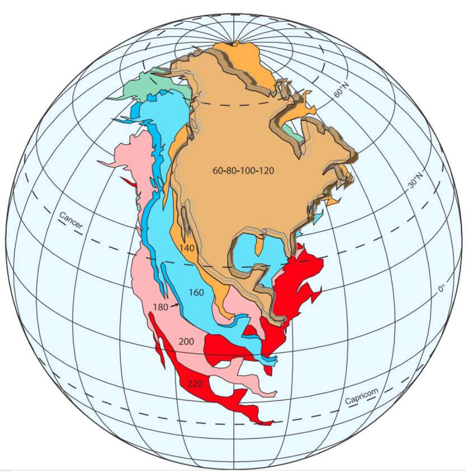

Kent and Irving (2010) figure 7.

Data handling note

We decided to do minimal data re-filtering to published detrital zircon data to test the effectiveness of a more "hands-off" approach to big-data interrogation. However, for the few samples that included no age transition for best age or discordance filter (e.g., Hagadorn et al., 2016), we preformed modest data manipulation. In these cases, we used 900 Ma for the $^{206}Pb/^{238}U$ and $^{206}Pb/^{207}Pb$ best age transition and < -10 and > 20% discordance filter.

Outliers

Of the 22 new detrital zircon samples that we present in this paper 4 contain outlier grains that pass filters (discussed above), but exhibit influences of Pb-loss and/or significant common Pb (inclusions). In general, samples exhibit high levels of discordance (mean: 61%), where the discordant ages trend along a line (a.k.a., discordia) that intersects with approximately middle Cenozoic ages on the condcordia (Fig. A1). We interpret these data to indicate Pb-loss and attribute this behavior to interaction with hydrothermal fluids during wide-spread volcanic activity during the late Paleogene in the North American western interior. The two samples (SJMT3 and BDJLS1) that each contain an outlier grain dated younger than the depositional age of the host rock exhibit this same trend (Fig. A2) and are interpreted to have experienced Pb-loss. The two samples that contain grains (SJMT1 and 2RFMMT3) with ages that are too old are a result of common Pb based on their isotopic compositions.

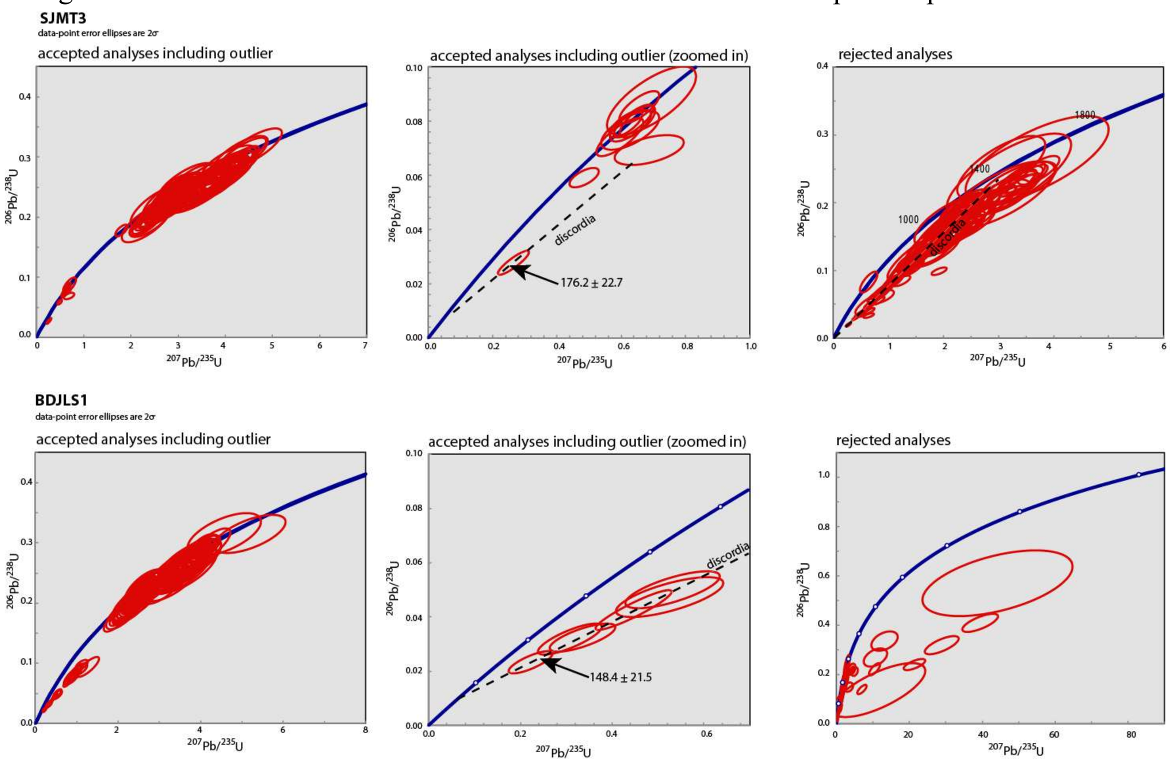

Figure A1. Concordia plots of accepted and rejected analyses containing analyses younger than depositional age of host rock (indicated by arrow and reported mean age and uncertainty).

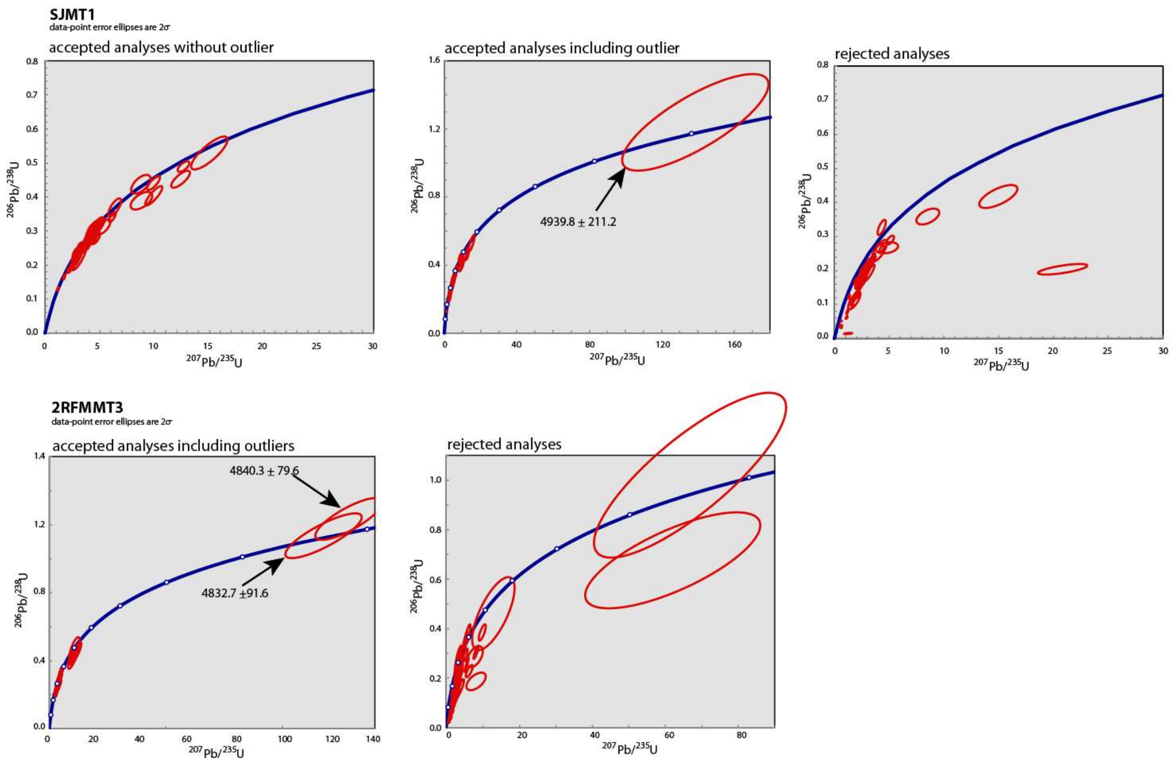

Figure A2. Concordia plots of accepted and rejected analyses containing analyses that are too old (indicated by arrow and reported mean age and uncertainty).

The outlier grains described above beg the question: Are the rest of the analyses reliable? In short, yes. While there are certainly other analyses within concordant grains that exhibit similar behavior to what is described above, the intrasample consistency between similar samples, both within the new ages reported here, as well as cited ages, provide a broad base of support for data fidelity. We do not remove the outlier analyses described above from modeling inputs in order to avoid a boutique approach. Rather, we thought it appropriate to flag these concerns while allowing the combination of modeling techniques to render outlier data inconsequential. In handling and interrogating big-data, there is almost certainly going to be problematic data contained within. However, an advantage to leveraging large data sets (i.e., $n \geq 10^3$) is that the few outliers are overwhelmed by the preponderance of reliable data. We believe that our approach demonstrates this phenomenon.

New detrital zircon sample descriptions

1CCT3: 36.3097, -106.33868

Mapped as the El Cobre Formation (Kempter et al., 2007), but is broadly considered Cutler Formation/Group (Ebert and Miall, 1991). Sample was collected in El Arroyo del Cobre, NM, at the base of a ~12 m medium-grain, reddish-brown trough cross-bedded sandstone. Sandstone exhibited an erosional base and contained meter-scale bar-forms (interpreted as laterally accreting). Sandstone also contained convolute-bedding, bioturbated zones, and abundant rip-up clasts.

1DCGT243: 38.69387, -108.97721

Mapped as Cutler Formation/Group, undivided (Williams, 1964). Collected outside of Gateway, CO from a 2 m fining upward, pebble to medium-grain sandstone, directly below the basal Moenkopi Formation gypsum bed. Gypsiferous cementation yields a highly friable rock and poorly exposed sedimentary structures. This area and stratigraphic position of the Cutler Formation is interpreted as White Rim Formation equivalent based on subsurface and outcrop correlation (Donald Rasmussen, personal communication).

1MHRCT201: 37.21699, -109.71693

Mapped as Halgaito Tongue of the Cutler Formation/Group (Haynes et al., 1972). Collected from a 2 m fine-grain, parallel laminated and minor-trough cross-bedded sandstone, interbedded with mottled red-brown mudstones containing abundant calcareous concretion nodules.

1MPT15: 37.751, -107.68359

Collected from Molas Formation (Evans and Reed, 2007) along Highway 550, west of Molas Lake. Sample was collected from an erosionally based, horizontally laminated with internal scouring, medium-grain, fining-upward to very fine-grain sandstone. Gravel-floaters at base of sandstone are chert and top of sandstone exhibits quartz sand-fracture fill.

2PCGT180: 38.71605, -108.91465

Mapped as Cutler Formation/Group, undivided (Williams, 1964) west of the Precambrian basement contact. Collected outside of Gateway, CO from a ~ 3 m structureless granule-size conglomerate with coarse to very-coarse grain sandstone matrix.

2RFMMT3: 39.67757, -107.69687

Mapped as the Maroon Formation (Tweto et al., 1978). Sample was collected from a ~3.8 m medium to coarse-grain, trough-cross-bedded, pinkish-gray sandstone.

2RFMMT383: 39.6645, -107.69758

Mapped as the State Bridge Formation (Tweto et al., 1978). Collected from a 1.3 m gray, fine-grain trough-cross-bedded sandstone that contains ripple cross-lamination, and is interbedded with red-brown rippled silty mudstones with climbing-ripple sandstone lenses. Cross-beds exhibit gray shale partings.

3FTCT166: 38.71164, -109.25915

Mapped as Cutler Formation/Group (Williams, 1964). Sample collected around Fisher Towers, east of Moab, UT. Sample is from a ~ 1.5 m mauve-colored, coarse-grain sandstone containing a pebbly base and pebble lags along ~ 80 cm cross-bed foresets. Sandstone is part of a ~ 5 m amalgamated, trough-cross-bedded sandstone interval.

4SMST778: 38.48116, -105.83811

Sample was collected from the middle of member 4 of the upper Sangre de Cristo Formation (Wallace et al., 1997; 2000), which is located east of Salida, CO and north of the Arkansas River. The sample is a trough-cross-bedded, coarse- to medium-grain with occasional granules, poorly sorted, angular, arkosic sandstone.

1CORT137: 38.50481, -109.66605

Mapped as Rico Formation (Williams, 1964), but is considered Cutler Formation/Group (Trudgill, 2011), as the Rico Formation is not current formation distinction. Collected from along the Colorado River, west of Moab, UT, in a ~ 15 m medium-grain, micaceous, mauve, trough-cross-bedded sandstone with abundant very coarse- to pebble-floaters, and erosional base.

AROM1: 38.48209, -105.91215

Mapped as Leadville Limestone (Taylor et al., 1975). Collected from ~ 1.5 m fine-grain, structureless, lense-shaped (~ 4 m long) quartzose sandstone. Associated with black micrite and intra-micrite that contain cm-scale sandstone lenses.

BDJ1ES1: 35.96477, -105.29186

Collected in the Espiritu Santo Formation, southeast, along strike of the base of measured section J1 in Baltz and Meyers, 1999. Location is on the north side of the Mora River, east of Mora, CO. The medium-grain, silica-cemented, quartz arenite does not exhibit observable sedimentary structures, but is interbedded with pervasively recrystallized limestone, and is close to the thrust-fault basement contact.

BDJLS1: 35.96218, -105.28649

Collected in the lower Sandia Formation, southeast, along strike of the middle of measured section J1, slightly upsection from Morrowan Brachiopod sample (USGS 27164-PC) in Baltz and Meyers, 1999. Location is on the north side of the Mora River, east of Mora, CO. Sample was comprised of coarse- to very coarse-grain, quartz-rich sandstone. Poor exposure of formation as associated gray shale beds form slope.

CT1: 38.10326, -105.60459

The sample site is mapped as undifferentiated Sangre de Cristo Formation (Hoy and Ridgeway, 2002), but we favor a Crestone Conglomerate assignment because of lithology and pervasive thrust-faulting in area (Hoy and Ridgeway, 2002). This is a lithologic distinction and both units in the area are considered Pennsylvanian-Permian (Hoy and Ridgeway, 2002). The sample site is located ~ 4.5 km east of Hermit Peak in the Sangre de Cristo Mountains. Sample is from a boulder conglomerate with a coarse-grain sandstone matrix. Sandstone is arkosic and gravel is comprised of igneous and metamorphic clasts.

FFM2: 38.5351, -104.88141

Collected from the upper Fountain Formation, west of Colorado Springs, CO. Sample is from a 2 m, erosionally based, coarse-grain, trough-cross-bedded sandstone containing abundant granules of quartz and feldspar.

SJMT1: 37.7503, -107.68007

Collected from a fine-grain, sandy limestone bed in the Leadville Limestone, north of the Molas Lake. Limestone is significantly recrystallized, and original depositional features are not present.

SJMT2: 37.745, -107.69656

Collected from lower Hermosa Group (Nair et al., 2018), most likely in the upper Pinkerton Formation or lower Paradox Formation. Sample collected from a very coarse- to coarse-grain, trough-cross-bedded sandstone with erosional base and is on top of a red-brown, clay-rich, fine-grain, structureless sandstone.

SJMT3: 37.62048, -107.8149

Collected from lower Paradox Formation (Gianniny and Miskell-Gerhardt, 2009) at the north end of the Hermosa Cliffs. Sample is from a ~ 10 m, multi-story, trough-cross-bedded, coarse-grain sandstone, and contained quart floater pebbles. Interbedded with fissile gray shale.

SJMT4: 37.51413, -107.82876

Collected from lower Honaker Trail Formation (Gianniny and Miskell-Gerhardt, 2009) at the north side of Goulding Creek/south end of the Hermosa Cliffs. Sample is from a micaceous, fine to medium-grain, trough cross-bedded sandstone that contained plant impressions along bedding planes.

SJMT7: 37.38501, -107.85325

Mapped as Cutler Formation (Stevens et al., 1974), south of Hermosa Lake, and north of Durango, CO. Sample collected from a 15 m amalgamated channel-complex that is medium-grain, trough cross-bedded sandstone.

SUPPLEMENTAL MATERIALS REFERENCES

Adams, R.D., 1980, Late Paleozoic tectonic and sedimentologic history of the Penasco Uplift, north-central New Mexico [M.A. thesis]: Houston, Rice University, 87 p.

Billingsley, G.H., 1999, Paleovalleys of the Surprise Canyon Formation in Grand Canyon, *in* G.H., Billingsley, and S.S., Beus, eds., Geology of the Surprise Canyon Formation of the Grand Canyon, Arizona: Museum of Northern Arizona Bulletin, 61, p. 17-52.

Blakey, R.C., 2009, Paleogeography and geologic history of the Western Ancestral Rocky Mountains, Pennsylvanian-Permian, southern Rocky Mountains and Colorado Plateau, *in* Houston, W.S., Wray, L.L., and Moreland, P.G., eds., The Paradox Basin Revisited – New Developments in Petroleum Systems and Basin Analysis: Rocky Mountain Association of Geologists Special Publication, p. 222-264.

Bowen, D.W. and Weimer, P., 2003, Regional sequence stratigraphic setting and reservoir geology of Morrow incised-valley sandstones (lower Pennsylvanian), eastern Colorado and western Kansas: American Association of Petroleum Geologists Bulletin, v. 87, no. 5, p. 781-815.

Brand, L., Wang, M., Chadwick, A., 2015, Data from: Global database of paleocurrent trends through the Phanerozoic and Precambrian, Dataset, https://doi.org/10.5061/dryad.hr0sp.

Conyers, L.B., 1975, Depositional environments of the Supai Formation in Central Arizona, [M.S. thesis]: Arizona State University, 86 p.

Dickinson, W.R., 2018, Tectonosedimentary relations of Pennsylvanian to Jurassic strata on the Colorado Plateau: The Geological Society of America Special Paper, v. 533, p. 1-184.

Dickinson, W.R., and Gehrels, G.E., 2008, U-Pb ages of detrital zircons in relation to paleogeography: Triassic paleodrainage networks and sediment dispersal across southwest Laurentia. Journal of Sedimentary Research, v. 78, p. 745-764.

Eberth, D.A., and Mail, A.D., 1991, Stratigraphy, sedimentology and evolution of a vertebrate-bearing, braided to anastomosed fluvial system, Cutler Formation (Permian-Pennsylvanian), north-central New Mexico: Sedimentary Geology, v. 72, p.225-252.

Evans, J.E., and Reed, J.M., 2007, Integrated loessite-paleokarst depositional system, early Pennsylvanian Molas Formation, Paradox Basin, southwestern Colorado, U.S.A.: Sedimentary Geology, v.195, p. 161-181.

Ewing, T.E., 2009, The ups and downs of Sabine Uplift and Gulf of Mexico Basin: Jurassic basement blocks, Cretaceous thermal uplifts, and Cenozoic: Gulf Coast Association of Geological Societies Transactions, v. 59, p. 253-269.

Gehrels, G.E., Blakey, R., Karlstrom, K.E., Timmons, J.M., Dickinson, B., and Pecha, M., 2011, Detrital zircon U-Pb geochronology of Paleozoic strata in the Grand Canyon, Arizona: Lithosphere, v. 3, no. 3, p. 183-200.

Geslin, J.K., 1998, Distal Ancestral Rocky Mountains tectonism: Evolution of the Pennsylvanian-Permian Oquirrh-Wood River Basin, southern Idaho: Geological Society of America Bulletin, v. 110, no. 5, p.644-663.

Hagadorn et al., 2016

Williamson, C.R., and Harms, J.C., 1988, Deep-water density current deposits of Delaware Mountain Group (Permian), Delaware Basin, Texas and New Mexico: American Association of Petroleum Geologists Bulletin, v. 72, p. 299-317.

Haynes, D.D., Vogel, J.D., and Wyant, D.G., 1972 Geology, structure, and Uranium deposits of the Cortez Quadrangle, Colorado and Utah: United States Geological Survey, Miscellaneous Investigations Series, Map I-629, scale 1:250,000.

Johnson, S.Y., 1987, Sedimentology and paleogeographic significance of six fluvial sandstone bodies in the Maroon Formation, Eagle Basin, northwest Colorado: United States Geological Survey Bulletin 1787-A, p. 1-18.

Kempter, K., Zeigler, K., Koning, D., and Lucas, S., 2007, Preliminary geologic map of the Canjilon SE Quadrangle, Rio Arriba County, New Mexico: New Mexico Bureau of Geology and Mineral Resources, OF-GM 150, scale 1:24,000.

Kent, D.V. and Irving, E., 2010, Influence of inclination error in sedimentary rocks on the Triassic and Jurassic apparent pole wander path for North America and implications for Cordilleran tectonics: Journal of Geophysical Research, v. 115, p. 1-25.

Lawton, T.F., Buller, C.D., and Parr, T.R., 2015, Provenance of a Permian erg on the western margin of Pangea: Depositional system of Kungurian (late Leonardian) Castle Valley and White Rim sandstones and subjacent Cutler Group, Paradox, Utah, USA: Geosphere, v. 11, no. 5, p. 1-32.

Lawton, T. F., Cashman, P. H., Trexler, J. H., and Taylor, W. J., 2017, The late Paleozoic Southwestern Laurentian Borderland: Geology, v. 45, no. 8, p. 675-678.

Lawton, T.F., Ruiz Urueña, J., E., Solari, L.A., Terrazas, C.T., Jauarez-Arriaga, Edgar, and Ortega-Obregón, Carlos, 2018, Provenance of Upper Triassic–Middle Jurassic strata of the Plomosas uplift, east-central Chihuahua, Mexico, and possible sedimentologic connections with Colorado Plateau depositional systems: Geological Society of America Special Paper, 540, p. 481-507.

Leary, R. J., Umhoefer, P., Smith, M. E., and Riggs, N., 2017, A three-sided orogen: A new tectonic model for Ancestral Rocky Mountain uplift and basin development: Geology, v. 45, no. 8, p. 735-738.

Loope, D.B., Steiner, MB, Rowe, C.M., and Lancaster, N., 2004, Tropical westerlies over Pangaean sand seas: Sedimentology, v. 51, p. 315-322.

McKee, E. D., 1940, Three types of cross-lamination in Paleozoic rocks of northern Arizona, American Journal of Science: v. 238, p. 811-824.

Nair, K., Singleton, J., Holm-Denoma, C., and Egenhoff, S., 2018, Detrital zircon geochronology of Pennsylvanian-Permian strata in Colorado: Evidence for Appalachian-derived sediment and implications for timing of Ancestral Rocky Mountains uplift: The Mountain Geologist, v. 55, n. 3, p.119-140.

Opdyke, N.D., and Runcorn, S.K., 1960, Wind direction in the western United States un the Late Paleozoic: Bulletin of Geological Society of America, v. 71, p. 959-972.

Rea, D.K., 1967, Stratigraphy of the red chert-pebble conglomerate in the Earp Formation, southeastern Arizona, [M.S. thesis]: Tucson, University of Arizona, 116 p.

Riggs, N.R., Lehman, T.M., Gehrels, G.E., and Dickinson, W.R., 1996, Detrital zircon link between headwaters and terminus of the upper Triassic Chinle-Dockum paleoriver system: Science, v. 273, no. 5271, p. 97-100.

Shaver, R.H., Ault, C.H., Burger, A.M., Carr, D.D., Droste, J.B., Eggert, D.L., Gray, H.H., Harper, D., Hasenmueller, N.R., Hasenmueller, W.A., Horowitz, A.S., Hutchinson, H.C., Kieth, B., Keller, S.J., Patton, J.B., Rexroad, C.B., and Weir, C.C., 1986, Compendium of Paleozoic rock-unit stratigraphy in Indiana – a revision: Indiana Geological Survey Bulletin 59, 203 p.

Soegaard, K., and Caldwell K.R., 1990, Depositional history and tectonic significance of alluvial sedimentation in the Permo–Pennsylvanian Sangre de Cristo Formation, Taos trough, New Mexico: New Mexico Geological Society Guidebook, 41st Field Conference, p. 277–289.

Soreghan, G.S., and Soreghan, M.J., 2013, Tracing clastic delivery to the Permian Delaware Basin, U.S.A.: Implications for paleogeography and circulation in westernmost equatorial Pangea: Journal of Sedimentary Research, v. 83, p. 786-802.

Soreghan, M.J., Heavens, N., Soreghan, G.S., Link, P.J., and Hamilton, M.A., 2014, Abrupt and high-magnitude changes in atmospheric circulation recorded in the Permian Maroon Formation, tropical Pangaea: geological Society of Americ Bulletin, v. 126, No. ¾, p. 569-584.

Stevens, T.A., Lipman, P.W., Hail, W.J., Barker, F., and Luedke, 1974, Geologic map of the Durango Quadrangle, southwestern Colorado: United States Geological Survey, Miscellaneous Investigations Series, Map I-764, scale 1:250,000.

Sundell, K.E., and Saylor, J.E., 2017, Unmixing detrital geochronology age distributions: Geochemistry, Geophysics, Geosystems, v. 18, p. 1-15.

Sweet, D.E., and Soreghan, G.S., 2010, Late Paleozoic tectonics and paleogeography of the ancestral Front Range: Structural, stratigraphic, and sedimentologic evidence from the Fountain Formation (Manitou Springs, Colorado): Geological Society of America Bulletin, v. 122, no. 3-4, p. 575-594.

Taylor, R.B., Scott, G.R., and Wobus, R.A., 1975, Reconnaissance geologic map of the Howard Quadrangle, central Colorado: United States Geological Survey, Miscellaneous Investigations Series, Map I-892, scale 1:62,500.

Trexler, J.H., Cashman, P.H., Snyder, W.S., and Davydov, V.I., 2004, Late Paleozoic tectonism in Nevada: Timing, kinematics, and tectonic significance: Geological Society of America Bulletin, v. 116, no. 5/6, p. 525-538.

Trudgill, B.D., 2011, Evolution of salt structures in the northern Paradox Basin: Controls on evaporite deposition, salt wall growth and supra-salt stratigraphic architecture: Basin Research, v.23, p. 208-238.

Tweto, O., Moench, R.H., and Reed, J.C., 1978, Geologic map of the Leadville 1° x 2° Quadrangle, Northwestern Colorado: United States Geological Survey, Miscellaneous Investigations Series, Map I-999, scale 1:250,000.

Wallace C.A., Cappa, J.A., and Lawson, A.D., 1997, Geologic map of Salida East Quadrangle, Chaffee and Fremont counties, Colorado: Colorado Geological Survey, Open-File Report 97-6 scale 1:24,000.

Wallace, C.A., Apeland, A.D., and Cappa, J.A., 2000, Geologic map of the Jack Hill Mountain Quadrangle, Fremont County, Colorado: Colorado Geological Survey, Open-File Report 00-1, scale 1:24,000.

Wang, W., and Bidgoli, T.S., 2019, Detrital zircon geochronologic constraints on patterns and drivers of continental-scale sediment dispersal in the Late Mississippian. Geochemistry, Geophysics, Geosystems, v. 20, p. 5522–5543.

Webster, G.D., and Houck, K.J., 1998, Middle Pennsylvanian, late Atokan-early Desmoinesian echinoderms from an intermontane basin, the Central Colorado Trough: Journal of Paleontology, v. 72, p. 1054-1072.

Whitmeyer, S.J., and Karlstrom, K.E., 2007, Tectonic model for the Proterozoic growth of North America: Geosphere, v. 3, no. 4, p. 220-259.

Williams, P.L., 1964, Geology, structure, and Uranium deposits of the Moab Quadrangle, Colorado and Utah: United States Geological Survey, Miscellaneous Investigations Series, Map I-360, scale 1:250,000.

Willis, G.C., 1967, Influence of local structures on sedimentary cycles of Late Pennsylvanian beds of the Sacramento Mountains, Otero County, New Mexico, *in* Elam, J.G. and S. Chuber *eds.,* Cyclic sedimentation in the Permian Basin, Symposium, West Texas, p. 100-110.

Ye, H., Royden, L., Burchfield, C., and Schuepbach, M., 1996, Late Paleozoic deformation of interior North America: The Greater Ancestral Rocky Mountains: American Association of Petroleum Geologists Bulletin, v. 80, no. 9, p. 1397-1423.